Electronic supporting information

Two-Photon Active Chevron-Shaped Type I Photoinitiator Designed for 3D Stereolithography.

Ruchun Zhou[1], Jean-Pierre Malval[2], Ming Jin[1], Arnaud Spangenberg[2], Haiyan Pan[1], Decheng Wan[1], Fabrice Morlet-Savary[2], Stephan Knopf[2].

[1]School of Materials Science and Engineering, Tongji University, 4800 Caoan Road, Shanghai, 201804, P.R. China
[2]Institute de Science des Matériaux de Mulhouse, UMR CNRS 7361, Université de Haute-Alsace, 15 rue Jean Starcky, Mulhouse, 68057, France

Correspondence to:
M. Jin (e-mail: mingjin@tongji.edu.cn), J.P. Malval (e-mail: jean-pierre.malval@uha.fr)

CONTENTS

1. Figures and Tables.

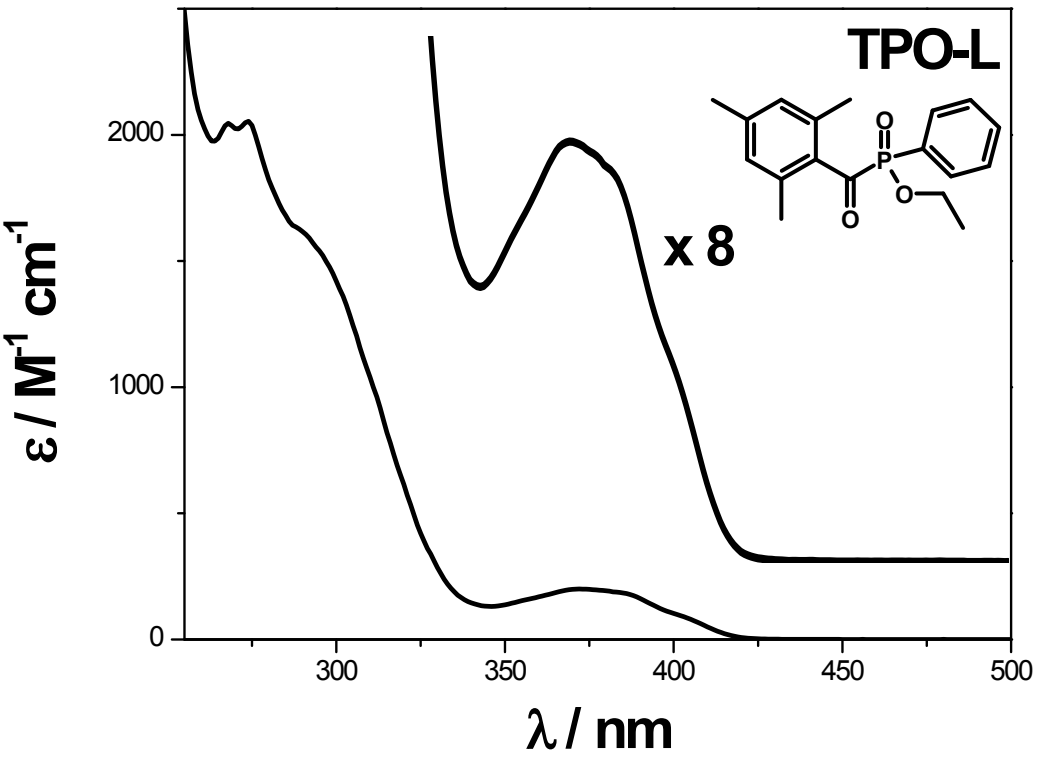

Figure S1. Molecular structure and absorption spectrum of **TPO-L** in acetonitrile.

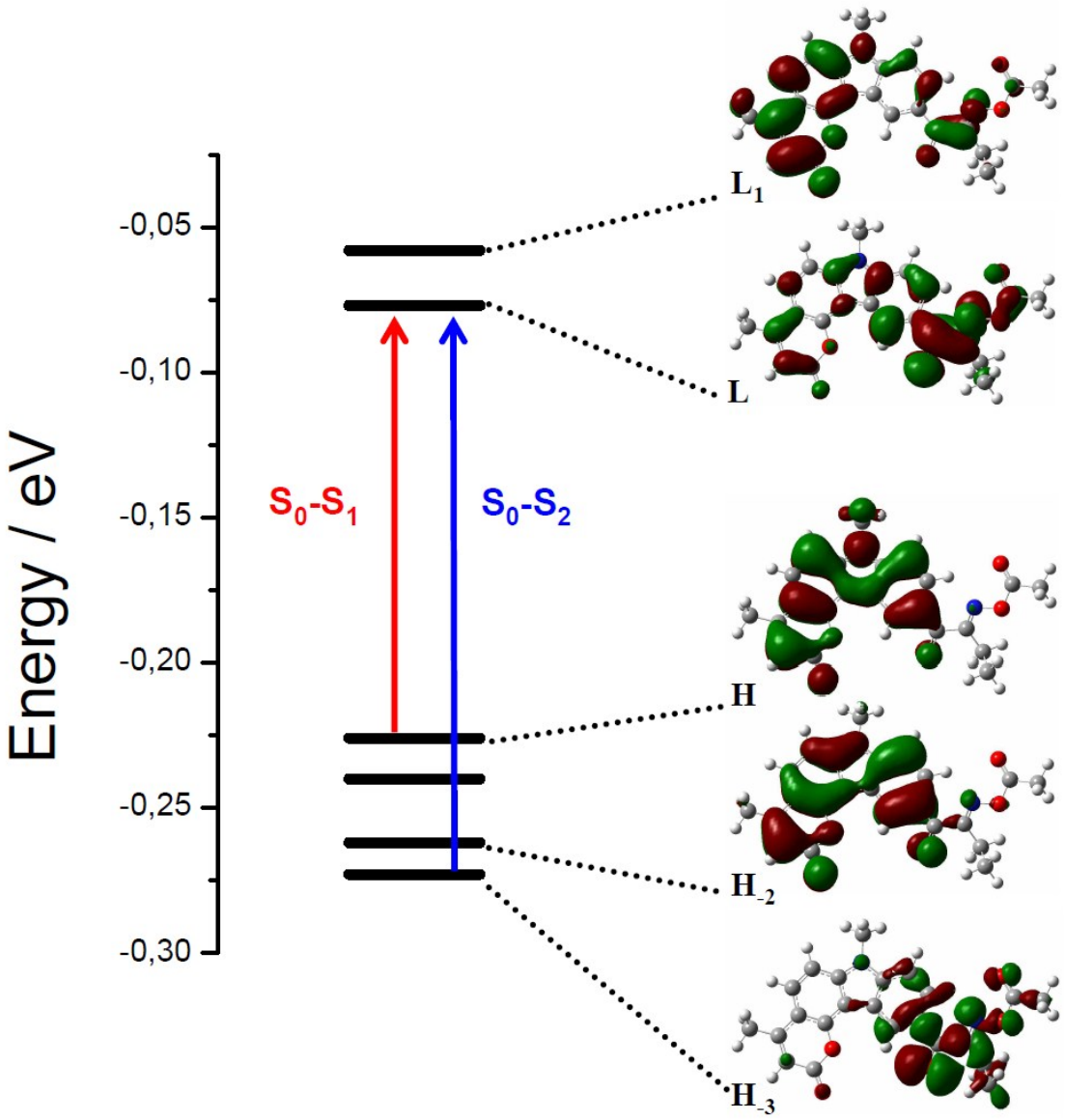

Figure S2. Frontier molecular orbitals (MO) diagrams of **OXE** with its two lowest energy S_0-S_1 S_0-S_2 transitions.

Experimental	**Theoretical**		
λ_{abs} (ε_{abs}) nm (10^3 M^{-1} cm^{-1})	λ_{abs} nm	f	Main transitions (fraction)
374 (16.6), 300 (22.9), 273 (30.4)	363	0.2254	$H \rightarrow L(1)$
	349	0.0154	$H_{-3} \rightarrow L(0.87)$
	340	0.0223	$H_{-1} \rightarrow L(0.86)$
	312	0.1862	$H \rightarrow L_1(0.86)$
	302	0.0122	$H_{-1} \rightarrow L_1(0.61)$ // $H \rightarrow L_2(0.36)$
	283	0.1598	$H_{-1} \rightarrow L_1(0.74)$ // $H_{-2} \rightarrow L(0.11)$
	281	0.0602	$H_{-2} \rightarrow L(0.89)$
	260	0.4053	$H_{-1} \rightarrow L_2(0.76)$ // $H \rightarrow L_3(0.12)$
	258	0.0130	$H_{-9} \rightarrow L$ (0.52) // $H_{-5} \rightarrow L$ (0.34)
	253	0.0282	$H_{-2} \rightarrow L_1(0.97)$
	243	0.2944	$H \rightarrow L_3(0.67)$ // $H_{-2} \rightarrow L_2(0.17)$

Table S3. Absorption properties of **OXE** in acetonitrile and corresponding TD-DFT data (TD-DFT-PBE0/6-31G+(d,p))

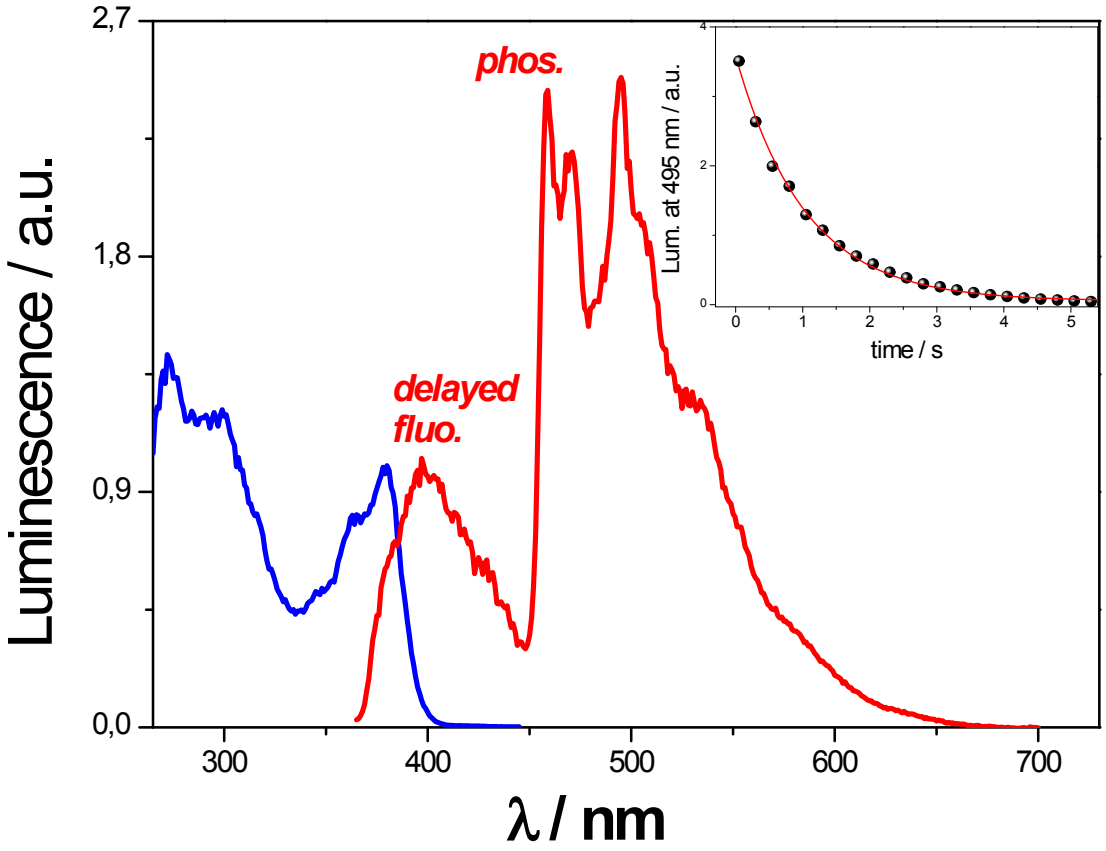

Figure S4. Low temperature excitation and emission spectra of **OXE** in glassy matrix of EtOH (77K). Inset : Decay profile of the phosophorescence recorded at 495 nm.

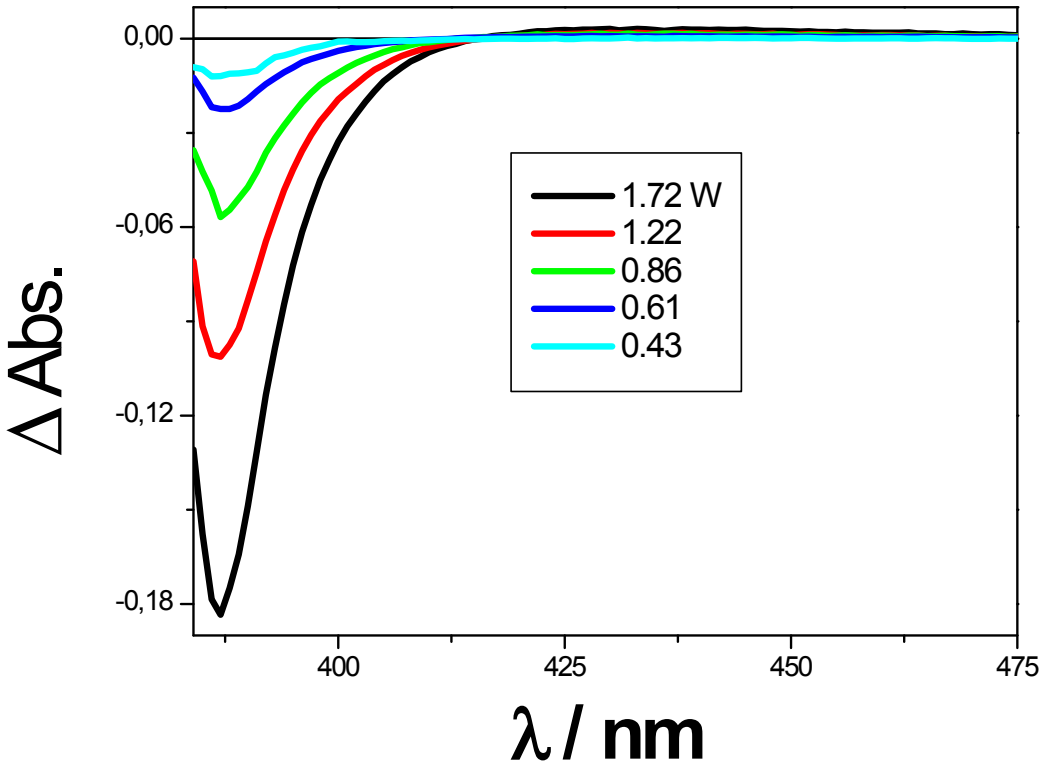

Figure S5. Differential absorption spectra at the lowest energy side of N_2-degassed ACN solutions of **OXE** (c: 1.3 mM) before and after irradiation at different two-photon excitation powers (λ_{irr} : 730 nm, Δt_{irr} = 20 min). Distinctive fresh **OXE** samples (i.e. 2 ml from a stock solution) were used for each excitation power.

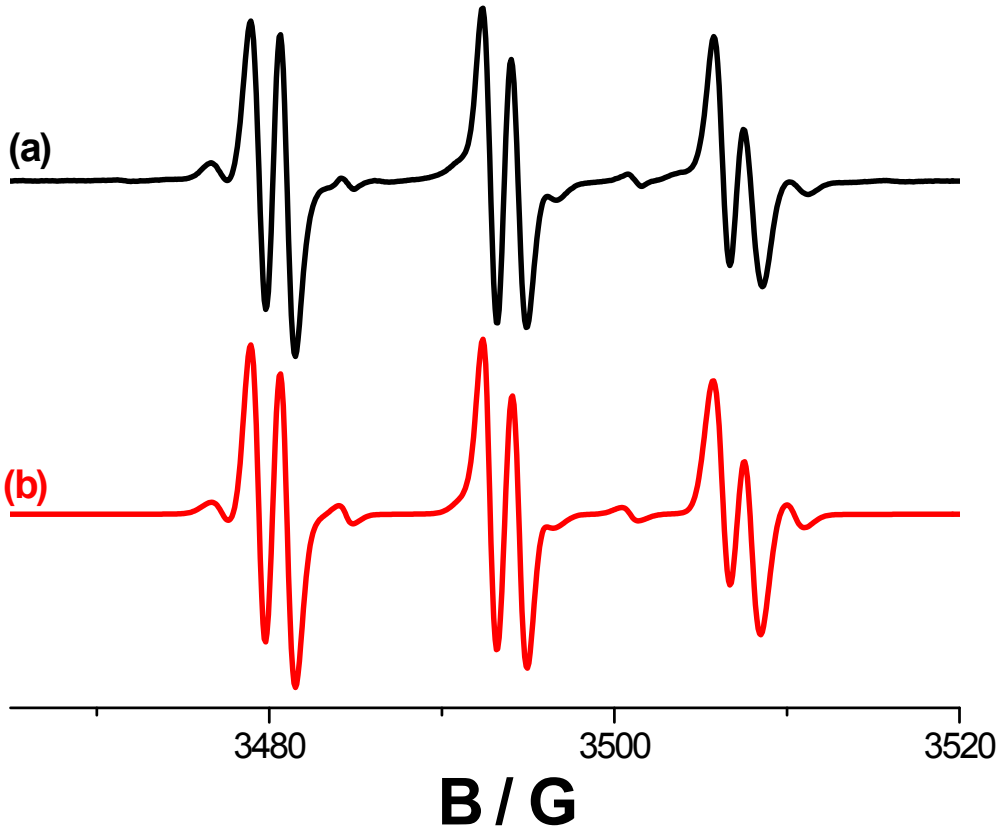

Figure S6. ESR spectrum of spin trap adduct generated after irradiation of **OXE** at 365 nm in presence of PBN. (Solvent: *tert*-butyl benzene) (b) Simulated spectrum.

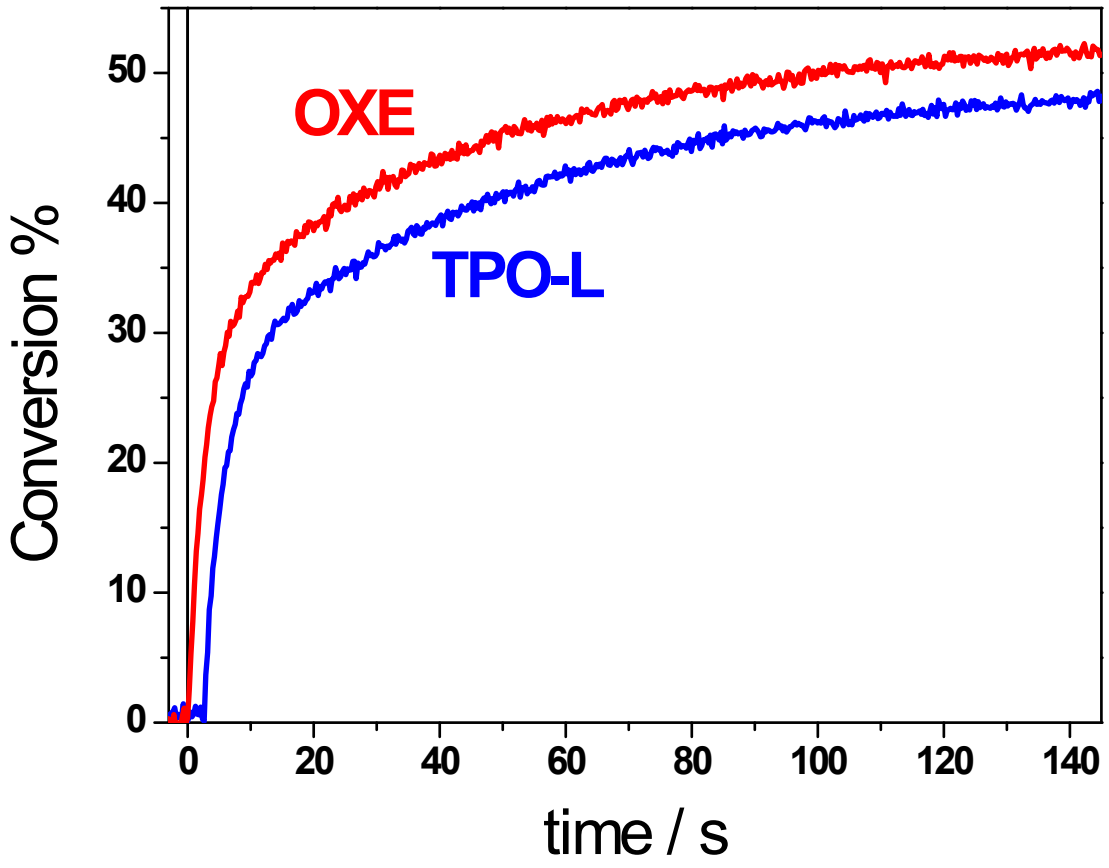

Figure S7. Photopolymerization profiles of isomolar formulations of **TPO-L** and **OXE** (2.5 mM) in pentaerythritol triacrylate (PETIA) irradiated at 365 nm (P = 1.5 mW cm^{-2})

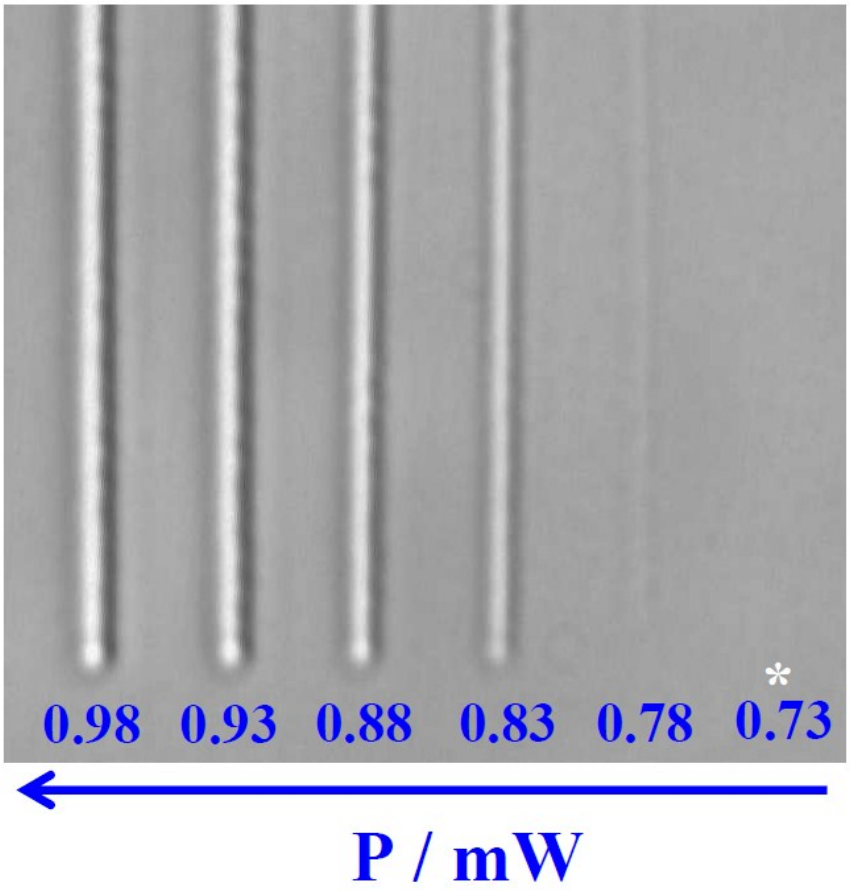

Figure S8. Two-photon polymerized lines fabricated for distinctive laser excitation powers (λ_{ex} = 800 nm, τ_{exp} = 4 ms). The star pictogram indicates the corresponding value of P_{th} at 800 nm. Formulation: Triacrylate resin (PETIA) mixed with **OXE** (2.5 mM).

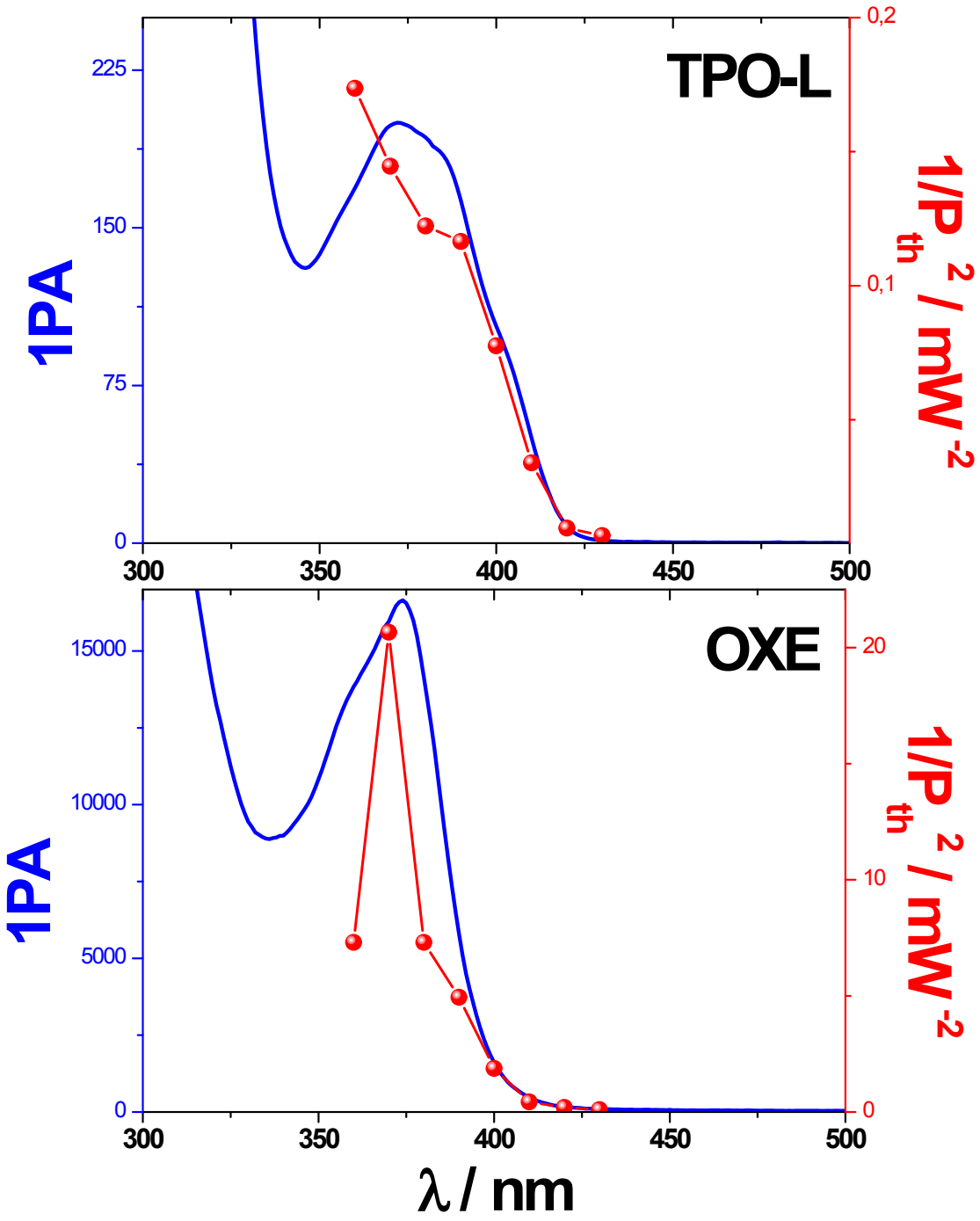

Figure S9. 1PA spectra of the photoinitiators in ACN (full lines) and 2PA action polymerization spectra (circles) of triacrylate formulations containing the photoinitiators at isomolar concentration (2PA spectra are plotted against half the $\lambda_{exc.}$)

2. Materials and General Characterization Methods.

Materials and general methods. All chemicals for synthesis were purchased from Energy Chemical or Sinopharm Chemical Reagent Co., Ltd.; TCI; or J&K Chemical, and they were used without further purification unless otherwise specified. All the solvents employed were Aldrich, Fluka or Merck spectroscopic grade. Pentaerythritol triacrylate (PETIA) monomer was purchased from Sartomer. Lucirin **TPO-L** was purchased from BASF (Ludwigshafen, Germany).

^{1}H NMR and ^{13}C NMR spectra were recorded on a Bruker 400M NMR spectrometer with $CDCl_3$ or d_6-DMSO as solvent and chemical shifts were reported in parts per million (ppm), which downfield from the Me_4Si resonance, used as the internal standard. Mass spectra were recorded on a Micromass GCT.

Steady-state absorption and luminescence spectra. The absorption measurements were carried out with a Perkin Elmer Lambda 2 spectrometer. The phosphorescence measurements were performed using the FluoroMax-4 spectrofluorometer which is equipped with a Xe-pulsed lamp operating at up to 25 Hz. Luminescence measurements were performed in ethanol at 77 K. The samples are placed in a 5-mm diameter quartz tube inside a Dewar filled with liquid nitrogen.

Actinometry. The determination of intersystem quantum yields (Φ_{ISC}) were performed on the basis of a phosphorescence method using triplet-triplet energy transfer between oxalate derivatives as energy donors and camphorquinone as energy acceptor (E_T = 2.23 eV). The details of the methodology have been previously described[1, 2]. The quantum yield measurements of the photolysis ($\Phi_{diss.}$) were carried out under continuous irradiation at 365 nm with an Hg-Xe lamp (LC 9588/01A from Hamamatsu) equipped with a band pass filter centred at 365 nm (A9616-07 from Hamamatsu). The progress of the reaction was monitored via the absorbance change at 365 nm using the transmitted actinide beam whose intensity was collected using a spectrometer (USB4000 from Ocean Optics). The intensity of the incident light (5.7×10^{-6} einstein/min at 365 nm) was measured with the ferrioxalate actinometer[3]. Experiments were performed at 25°C in N_2-degassed solutions of acetonitrile which were continuously stirred.

Photopolymerization. The photopolymerization was monitored *in situ* by real-time Fourier transformed infrared spectroscopy with a Thermo-Nicolet 6700 IR-spectrometer. The laminated formulations are sandwiched between two polypropylene films to minimize the inhibiting effect of oxygen. A round teflon spacer is used to maintain a constant thickness of 25 µm. The sample is then positioned between two BaF_2 pellets and irradiated using a 100 W Mercury-Xenon Lamp (LC 9588/02A from Hamamatsu) equipped with a band pass filter centred at 365 nm (A9616-07 from Hamamatsu). The conversion rates are obtained from the disappearance of the progressive vinyl C=C stretching vibration band at 1630 cm^{-1}.

ESR Spin Trapping (ESR-ST) Experiment. Electron spinning resonance spin trapping (ESR-ST) experiments carried out by a Bruker EMX-plus spectrometer (X-band). The radicals generated when exposed to LED light source (365nm) at room temperature under Argon and were trapped by phenyl N-tert-butylnitrone (PBN) in *tert*-butyl benzene.

Open-aperture Z-scan method. The two-photon absorption spectra were measured using open-aperture Z-scan method[4-6] with a femtosecond mode-locked Ti: Sapphire laser (Coherent, Chameleon Ultra II : pulse duration: 140 ± 20 fs; repetition rate: 80 MHz; wavelength range: 680-1080 nm). After passing through a beam expander (x 4), the laser beam is focused using an f = 15 cm lens and passed through a quartz cell (1 mm optical path length). The position of the sample cell is varied along the laser-beam direction (z-axis) using a Z-step motorized stage controlled by a computer. At constant incident excitation, the local power density within the sample is changed and the corresponding transmitted laser beam, *T(z)*, recorded with a silicon photodetector (Ophir PD300) is monitored in connection with the z-position of the cell. The on-axis peak intensity of the incident pulses at the focal point, I_0, ranged from 0.5 to 3 GW cm^{-2}. If we assume that the linear absorption of the sample is negligible at working wavelength and that the laser exhibits a Gaussian beam profile in space and time, the nonlinear absorption coefficient β can be calculated from the curve fitting to the experimental transmittance with the following equation:

$$T(z) = 1 - \frac{\beta l I_0}{2\sqrt{2}\left(1 + \left(\frac{z}{z_0}\right)^2\right)} \qquad (1)$$

Where z_0 is the coordinate along the propagation direction of the focal point of the beam, l the optical path length. The 2PA cross-section, δ, (in units of 1 GM : 10^{-50} cm^4 s $photon^{-1}$ $molecule^{-1}$) is then determined by using the relationship:

$$\beta = \frac{\delta N_A d}{h\nu} 10^{-3} \qquad (2)$$

Where h is the Planck constant, ν the frequency of the incident laser beam, N_A the Avogadro constant and d is the concentration of the chromophore (mol. L^{-1}). The rhodamine 6G in methanol[7] (16.2 ± 2.4 GM at 806 nm) was used for the calibration of our measurement technique). For instance, **Figure S10** depicts z-scan traces of **OXE** (7 x 10^{-2} M in CH_2Cl_2) at 720 nm for distinctive incident powers. The linear correlation between the variation of transmission (ΔT) and the incident power (inset **Figure S10**) confirms the two-photon absorption regime[6].

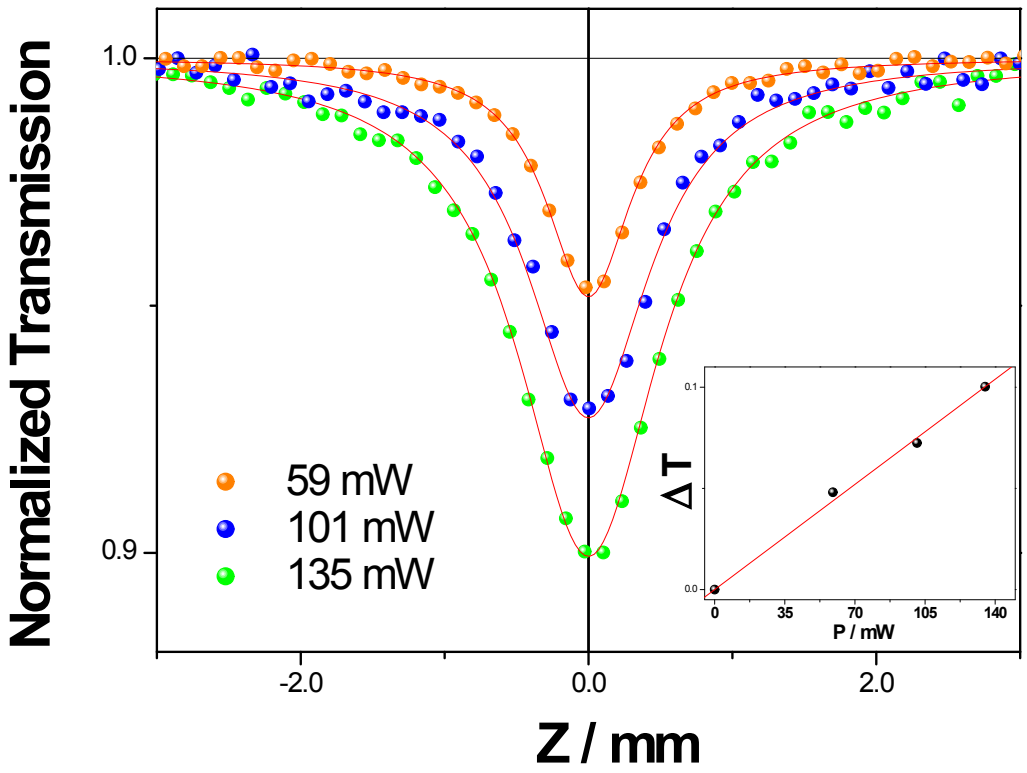

Figure S10 Z-scan traces of **OXE** in dichloromethane (7 x 10^{-2} M) at 720 nm for various excitation powers. On the basis of equation 1, the least squares fitted curves for each Z-scan trajectory are also reported. Inset: Transmittance variation *vs.* excitation power.

Since **OXE** undergoes a photolysis reaction upon two-photon excitation, each z-scan measurement was repeated three times per λ_{exc} using fresh **OXE** solutions. The resulting 2PA cross-sections were then averaged leading to an uncertainty of 15 % for the values of δ.

Microfabrication. The 3D lithographic microfabrication was carried out using a Zeiss Axio Observer D1 inverted microscope. The two-photon excitation was performed at 800 nm using respectively a mode-locked Ti: Sapphire oscillator (Coherent, Chameleon Ultra II: pulse duration: ~140 fs; repetition rate: 80 MHz). The incident beam was focused through a 0.65 NA objective (40 X) which leads to a radial spot size 600 nm at λ_{exc} = 800 nm ($1/e^2$ Gaussian). A drop of the resin is deposited on a cover slip which is mounted on a 3D piezoelectric stage allowing the translation relative to the laser focal point. The intensity of the entering laser is controlled with the use of an acousto optic modulator. The displacement of the sample and all photonic parameters (i.e. excitation power and irradiation times) are computer-controlled. The 3D microstructure is finally obtained by washing away the unexposed monomer resin using ethanol.

DFT calculations. The theoretical absorption spectrum has been computed based on Density Functional Theory (DFT) and Time-Dependent DFT (TDDFT). The overall computation strategy was defined as follows: First, to avoid long time computation, calculations have been done on **OXE** where the long hexyl branch was replaced by a methyl group. Then, after initial AM1 optimization calculations (vacuum), a subsequent optimization of the geometrical structure of **OXE** was carried out using the PBE0/6-31G+(d,p) level of calculation. (Note that PBE0 is a good functional for the description of photofunctional molecules[8]). Finally, the TDDFT vertical transitions have been computed using the same level of calculations. All calculations have been performed using GAUSSIAN 09 package[9].

ACKNOWLEDGMENTS

The authors acknowledge the meso-centre 'EQUIPEX@MESO' of Strasbourg University for access to High Performance Calculation resources.

3. Synthesis of OXE.

The synthetic route and characterization of immediate products and **OXE** were shown below (Scheme S1) and the ^{1}H NMR and ^{13}C NMR spectra were shown in Figures S11-15.

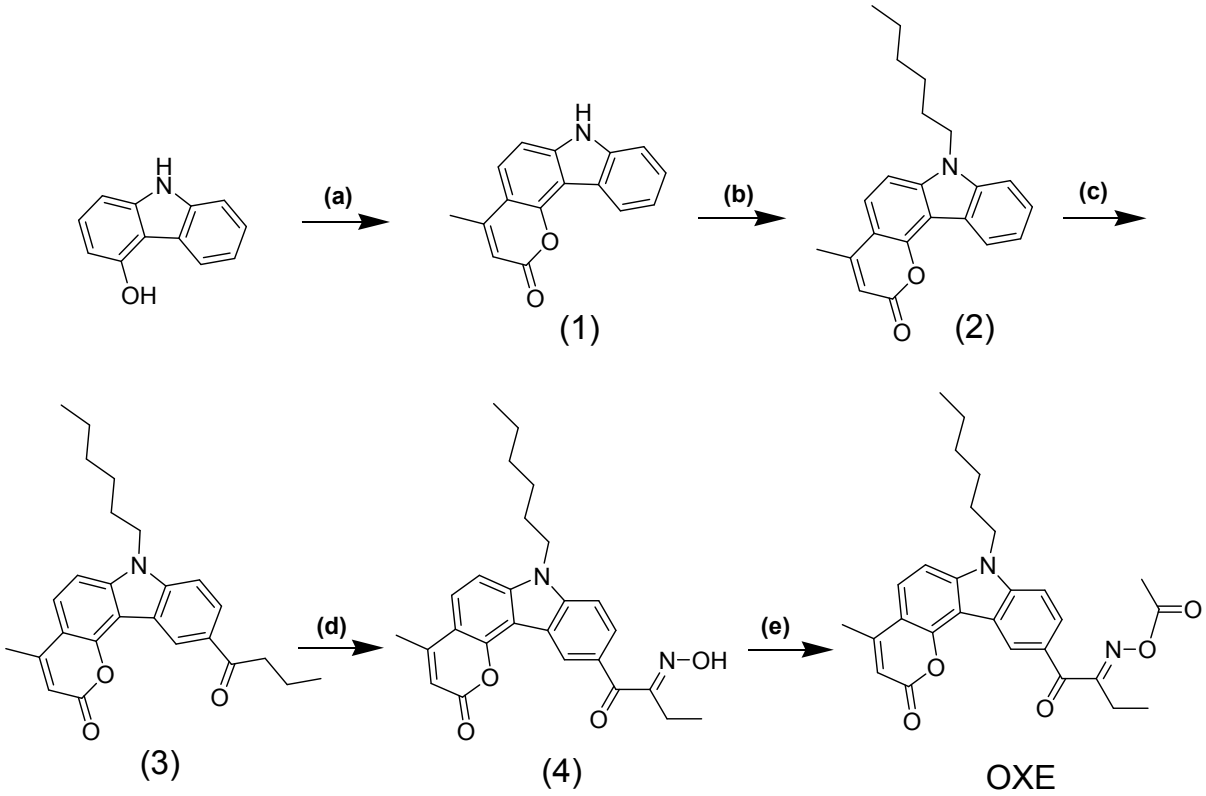

Scheme S1. Synthetic routes of the **OXE**. (a) Ethyl acetoacetate, anhydrous $BiCl_3$, 100 °C, 4h, N_2; (b) Bromohexane, K_2CO_3, Potassium iodide, 18-crown-6, DMF, 100 °C, 24h, N_2; (c) Anhydrous $AlCl_3$, butyryl chloride, dry CH_2Cl_2, 0-10 °C, 2h; (d) Conc. Hydrochloric acid, Isoamyl nitrite, THF, r.t. 5h; (e) acetic anhydride, triethylamine, dry CH_2Cl_2, 0-10 °C, 2h.

Synthesis of 4-methyl-pyrano[*3,2-c*]carbazol-2(*7H*)-one (1)

A mixture of 4-hydroxycarbazole (3.83 g, 20 mmol), ethyl acetoacetate (2.90 g, 22 mmol) and anhydrous $BiCl_3$ (0.60 g, 20 mmol) was heated at 90°C for 4 h under N_2. Then the reaction mixture was cooled down to room temperature and poured into 40 mL ethanol. The crude product was filtered off, washed with ethanol and dried in vacuo. The gray white product (1) was used for the next step without purification, 2.89 g, yield: 55.4%. ^{1}H NMR (400 MHz, d_6-DMSO) δ = 11.88 (s, 1H), 8.30 (d, *J*=7.8 Hz, 1H), 7.70 (d, *J*=8.6 Hz, 1H), 7.59 (d, *J*=8.1 Hz, 1H), 7.47 (dd, *J*=13.5 Hz, 7.9 Hz, 2H), 7.31 (t, *J*=7.4 Hz, 1H), 6.24 (s, 1H), 2.47 (s, 3H). ^{13}C NMR (101 MHz, d_6-DMSO) δ = 160.12, 154.76, 149.74, 142.42, 139.51, 126.00, 122.39, 122.16, 120.47, 120.07, 111.50, 110.92, 109.77, 109.34, 108.03, 18.83. MS (ESI MS) m/z: theor, 249.1; found, 250.1 ($[M + H]^+$ detected).

Synthesis of 7-hexyl-4-methylpyrano[3,2-c]carbazol-2(7H)-one (2)

Compound (1) (2.46 g, 10 mmol), 1-bromohexane (1.64 g, 10 mmol) and potassium carbonate (2.76 g, 20 mmol) were dissolved in 40 mL DMF in a flask fitted with a magnetic stirrer and condenser. Then a small amount of potassium iodide and 18-crown-6 were added as catalyst. The reaction was stirred for 24 h at 100 ˚C under N_2. The mixture was cooled to room temperature and poured into 400 mL water, the precipitated solid was collected and purified by column chromatography (SiO_2, petroleum ether/ethyl acetate, 4: 1, v/v) to obtain yellow product (2), 2.87 g, yield: 86.2%. ^{1}H NMR (400 MHz, $CDCl_3$) δ = 8.56 (d, *J*=7.8 Hz, 1H), 7.57 (d, *J*=8.7 Hz, 1H), 7.49 (t, *J*=8.2 Hz, 1H), 7.41 (d, *J*=8.2 Hz, 1H), 7.30 (t, *J*=7.1 Hz, 1H), 7.25 (d, *J*=7.5 Hz, 1H + $CDCl_3$), 6.14 (d, 1H), 4.28 (t, *J*=7.3 Hz, 2H), 2.46 (d, 3H), 1.89 – 1.79 (m, 2H), 1.36 – 1.22 (m, 6H), 0.84 (t, *J*=7.0 Hz, 3H). ^{13}C NMR (101 MHz, $CDCl_3$) δ = 161.72, 154.13, 150.60, 143.02, 140.29, 126.30, 124.05, 121.83, 121.27, 120.67, 111.77, 110.90, 110.50, 109.08, 105.71, 77.55, 77.43, 77.23, 76.91, 43.66, 31.71, 29.22, 27.09, 22.71, 19.57, 14.19. MS (ESI MS) m/z: theor, 333.4; found, 334.5 ($[M + H]^+$ detected).

Synthesis of 9-butyryl-7-hexyl-4-methylpyrano[3,2-c]carbazol-2(7H)-one (3)

Compound (2) (2.5 g, 7.5 mmol) and anhydrous $AlCl_3$ (2.01 g, 15 mmol) were added to a 100 mL-flask along with 15 mL anhydrous dichloromethane and the mixture was stirred at 0˚C for 10 minutes under N_2 atmosphere. Then the n-butyryl chloride (1.60 g, 15 mmol) dissolved in 5 mL of dichloromethane was added dropwise by syringe in 30 min and the reaction was finished after 2 h below 10 ^{o}C. The mixture was extracted with dichloromethane (3 × 100 mL), washed with water and the organic layer was dried with anhydrous sodium sulfate and concentrated under reduced pressure; the crude product was purified by column chromatography (SiO_2, petroleum ether/ethyl acetate, 4: 1, v/v) to obtain yellow product (3), 2.56g, yield: 84.7 %. ^{1}H NMR (400 MHz, $CDCl_3$) δ = 9.05 (d, *J*=1.4 Hz, 1H), 8.18 (dd, *J*=8.7 Hz, 1.7 Hz, 1H), 7.61 (d, *J*=8.7 Hz, 1H), 7.41 (d, *J*=8.7 Hz, 1H), 7.28 (d, *J*=8.7 Hz, 1H), 6.20 (s, 1H), 4.30 (t, *J*=7.3 Hz, 2H), 3.13 (t, *J*=7.2 Hz, 2H), 2.48 (s, 3H), 1.83 (dt, *J*=14.5 Hz, 7.3 Hz, 4H), 1.36 – 1.21 (m, 6H), 1.05 (t, *J*=7.4, 3H), 0.83 (t, *J*=7.0 Hz, 3H). ^{13}C NMR (101 MHz, $CDCl_3$) δ = 200.27, 161.10, 153.81, 150.51, 143.61, 142.87, 130.56, 126.51, 124.88, 122.55, 120.79, 112.54, 111.66, 110.87, 109.13, 106.04, 77.55, 77.44, 77.23, 76.91, 43.91, 40.49, 31.65, 29.22, 27.03, 22.68, 19.59, 18.25, 14.21, 14.16. HRMS (ESI MS) m/z: theor, 403.2; found, 404.4 ($[M + H]^+$ detected).

Synthesis of (E)-7-hexyl-9-(2-(hydroxyimino)butanoyl)-4-methylpyrano[3,2-c]carbazol-2(7H)-one (4)

Compound (3) (2.02 g, 5 mmol), hydrochloric acid (37%) (2.44 g, 25 mmol) and isoamyl nitrite (0.87 g, 7.5 mmol) were added to 10 mL THF. The mixture was stirred at room temperature for 5h and then poured into water, extracted with dichloromethane, dried with anhydrous sodium sulfate and concentrated under reduced pressure, the viscous product was washed in petroleum ether and the yellow solid (4) was separated out, filtration and used for the next step without purification, 1.17g, yield: 54.2 %. ^{1}H NMR (400 MHz, d_6-DMSO) δ = 12.21 (s, 1H), 8.83 (s, 1H), 8.08 (dd, *J*=8.7 Hz, 1.7 Hz, 1H), 7.81 (d, *J*=8.8 Hz, 1H), 7.76 (d, *J*=8.7 Hz, 1H), 7.64 (d, *J*=8.8 Hz, 1H), 6.31 (d, *J*=1.1 Hz, 1H), 4.46 (t, *J*=7.0 Hz, 2H), 2.67 (q, *J*=7.5 Hz, 2H), 2.50 (d, *J*=1.0 Hz, 3H + d_6-DMSO), 1.76 (dd, *J*=12.8 Hz, 6.7 Hz, 2H), 1.27 – 1.10 (m, 9H), 0.78 (t, *J*=7.0 Hz, 3H). ^{13}C NMR (101 MHz, d_6-DMSO) δ = 191.24, 159.77, 159.33, 154.61, 149.51, 143.23, 142.39, 129.19, 128.68, 125.27, 123.38, 119.58, 111.91, 110.59, 109.38, 109.16, 106.86, 42.93, 40.14, 39.93, 39.72, 39.51, 39.30, 39.09, 38.88, 30.89, 28.52, 25.93, 21.95, 18.83, 17.91, 13.81, 10.39. HRMS (ESI MS) m/z: theor, 432.5; found, 431.3 ($[M - H]^+$ detected).

Synthesis of OXE. (E)-10-(2-(acetoxyimino)butanoyl)-7-hexyl-4-methylpyrano[3,2-c]carbazol-2(7H)-one.

Compound (4) (0.43 g, 1 mmol) and dry triethylamine (0.57 g, 5mmol) were dissolved in 10 mL anhydrous dichloromethane. Then the acetic anhydride (0.29 g, 2.5mmol) dissolved in 5 mL of dichloromethane were added dropwise by syringe in 1 h. The flask was then stirred at room temperature for 2 h under N_2 atmosphere. The solution was subsequently washed with 2M HCl, sat. $NaHCO_3$, and sat. NaCl aqueous solutions and dried over Na_2SO_4. Then the crude product was purified chromatographically (SiO_2, petroleum ether/ ethyl acetate, 2: 1, v/v) to obtain aimed products (5), 0.34 g, yield: 71.7%. ^{1}H NMR (400 MHz, $CDCl_3$) δ = 9.07 (s, 1H), 8.18 (dd, *J*=8.7 Hz, 1.7 Hz, 1H), 7.55 (d, *J*=8.7 Hz, 1H), 7.34 (d, *J*=8.8 Hz, 1H), 7.25 (d, *J*=8.4 Hz, 1H + $CDCl_3$), 6.12 (s, 1H), 4.20 (t, *J*=7.2 Hz, 2H), 2.87 (q, *J*=7.6 Hz, 2H), 2.41 (d, *J*=0.4 Hz, 3H), 2.33 (s, 3H), 1.76 (dd, *J*=14.2 Hz, 7.1 Hz, 2H), 1.24 (t, *J*=7.6 Hz, 9H), 0.81 (t, *J*=7.0 Hz, 3H). ^{13}C NMR (101 MHz, $CDCl_3$) δ = 189.72, 168.96, 166.02, 160.71, 153.62, 150.25, 143.53, 143.45, 128.64, 128.19, 127.91, 122.88, 120.91, 112.61, 111.70, 110.58, 109.09, 106.24, 77.55, 77.43, 77.23, 76.91, 43.82, 31.60, 29.13, 26.91, 22.64, 21.51, 19.97, 19.49, 14.13, 10.76. HRMS (ESI MS) m/z: theor, 474.2155; found, 497.2053 ($[M + Na]^+$ detected), 513.1772 ($[M + K]^+$ detected).

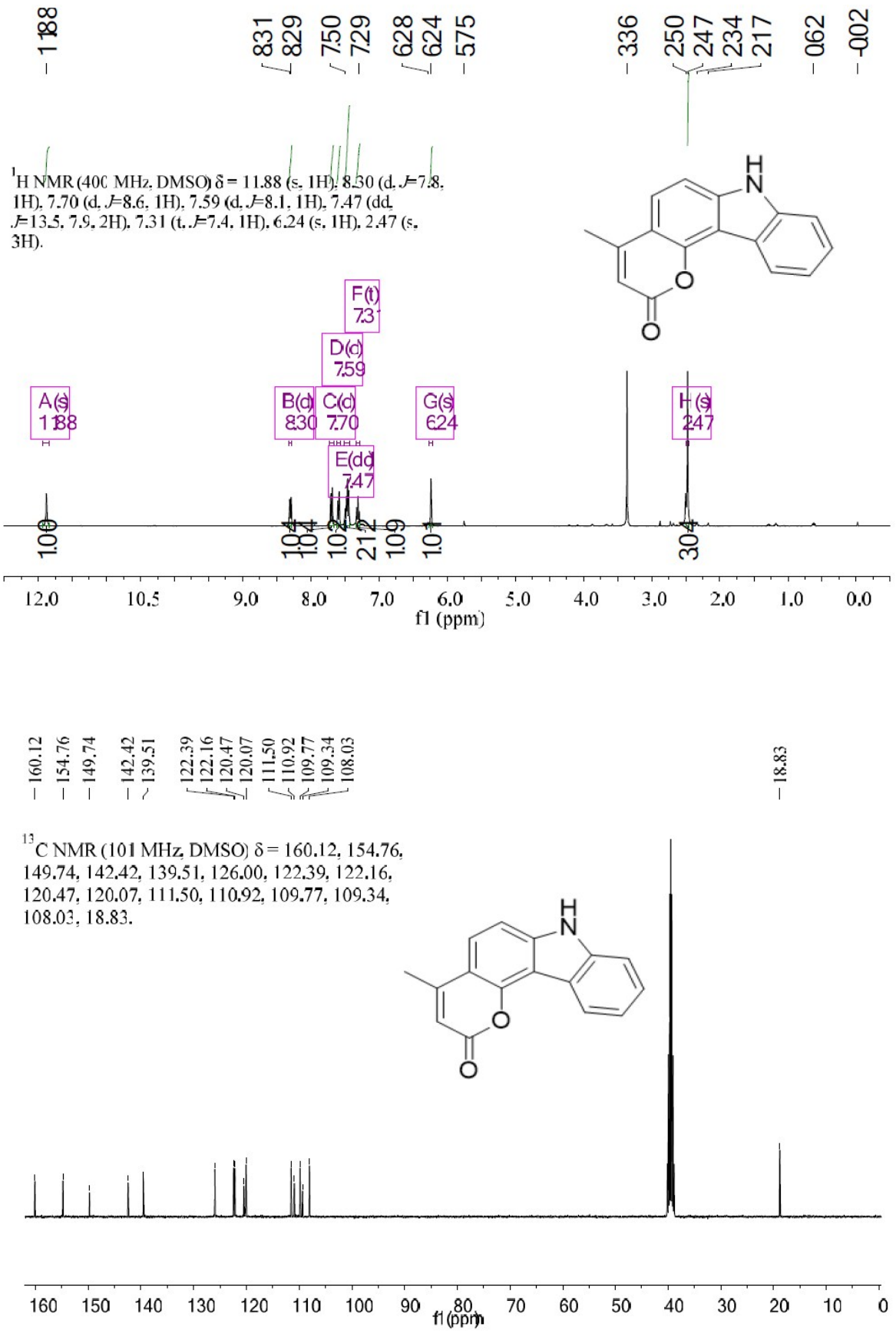

Figure S11. The ^{1}H and ^{13}C NMR spectra of compound (1) in d_6-DMSO.

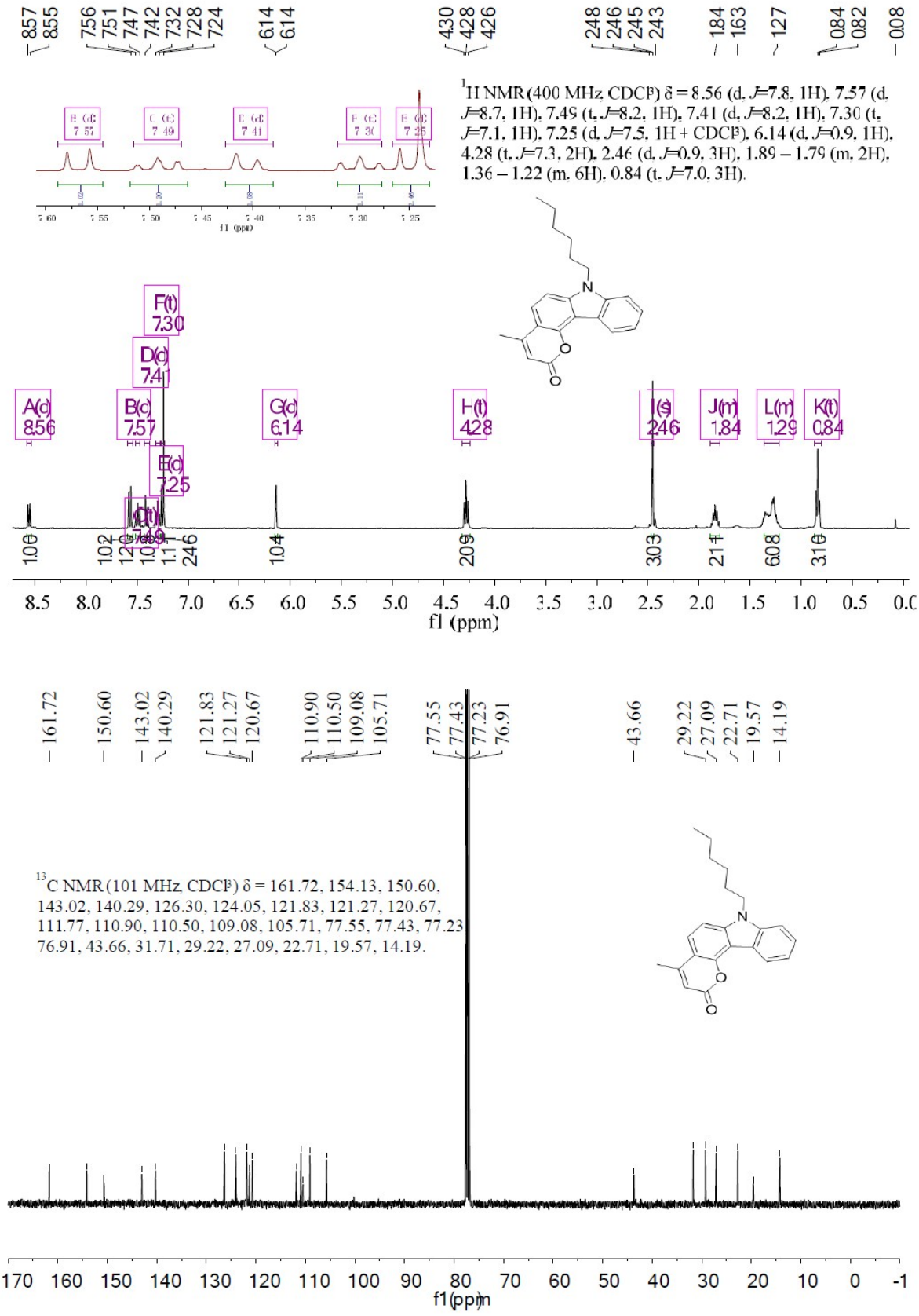

Figure S12. The ^{1}H and ^{13}C NMR spectra of compound (2) in $CDCl_3$.

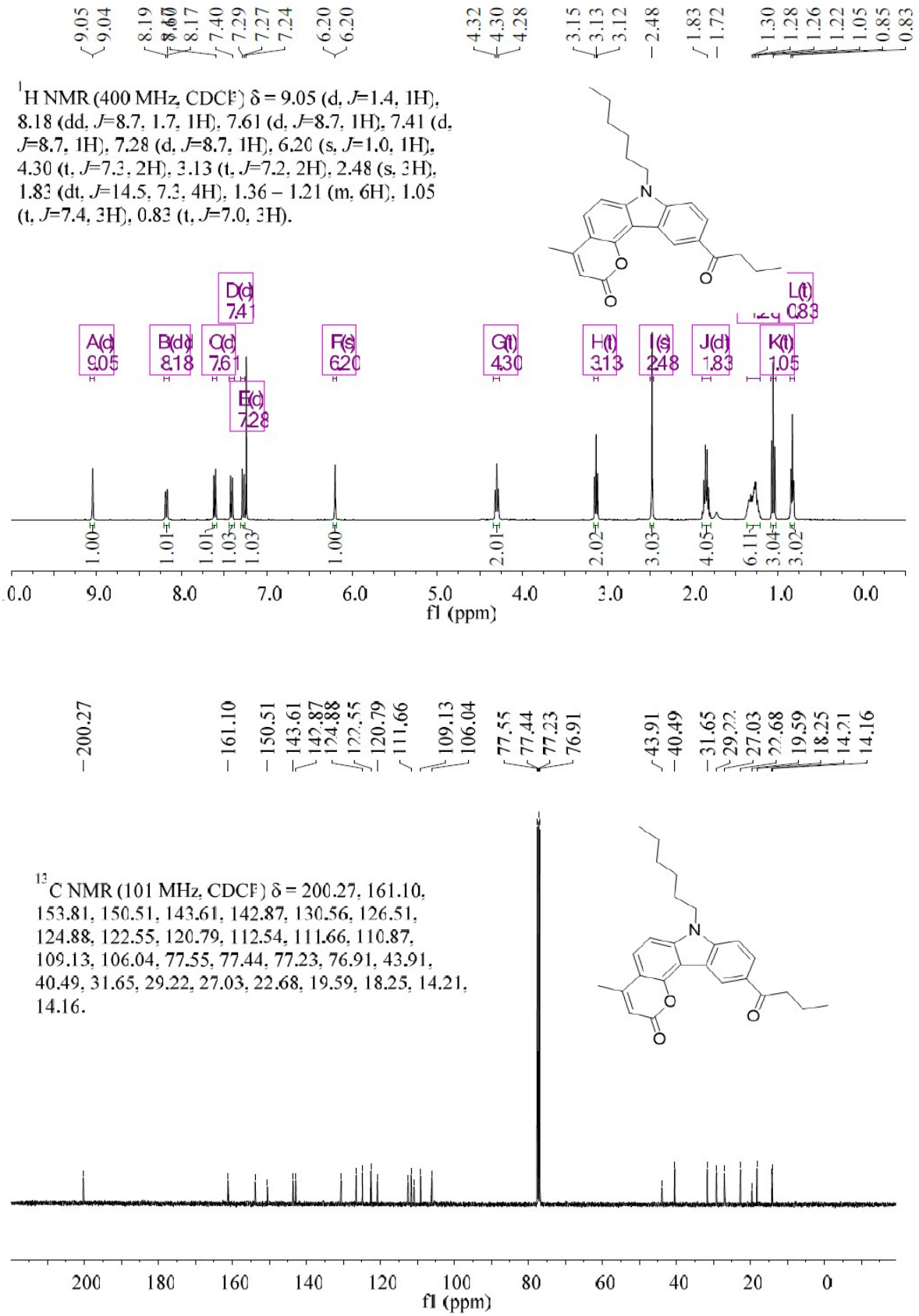

Figure S13. The ^{1}H and ^{13}C NMR spectra of compound (3) in $CDCl_3$.

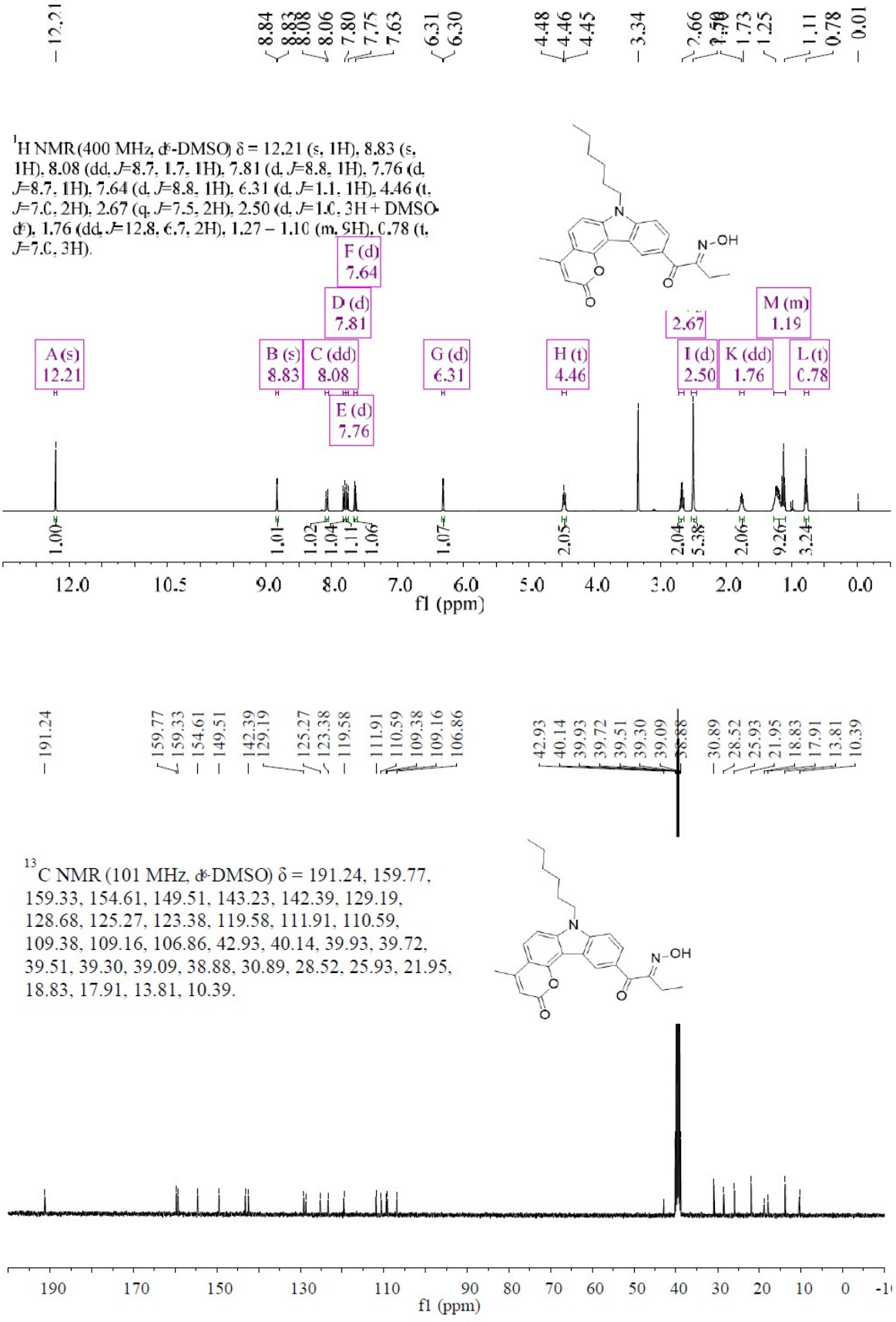

Figure S14. The ^{1}H and ^{13}C NMR spectra of compound (4) in d_6-DMSO.

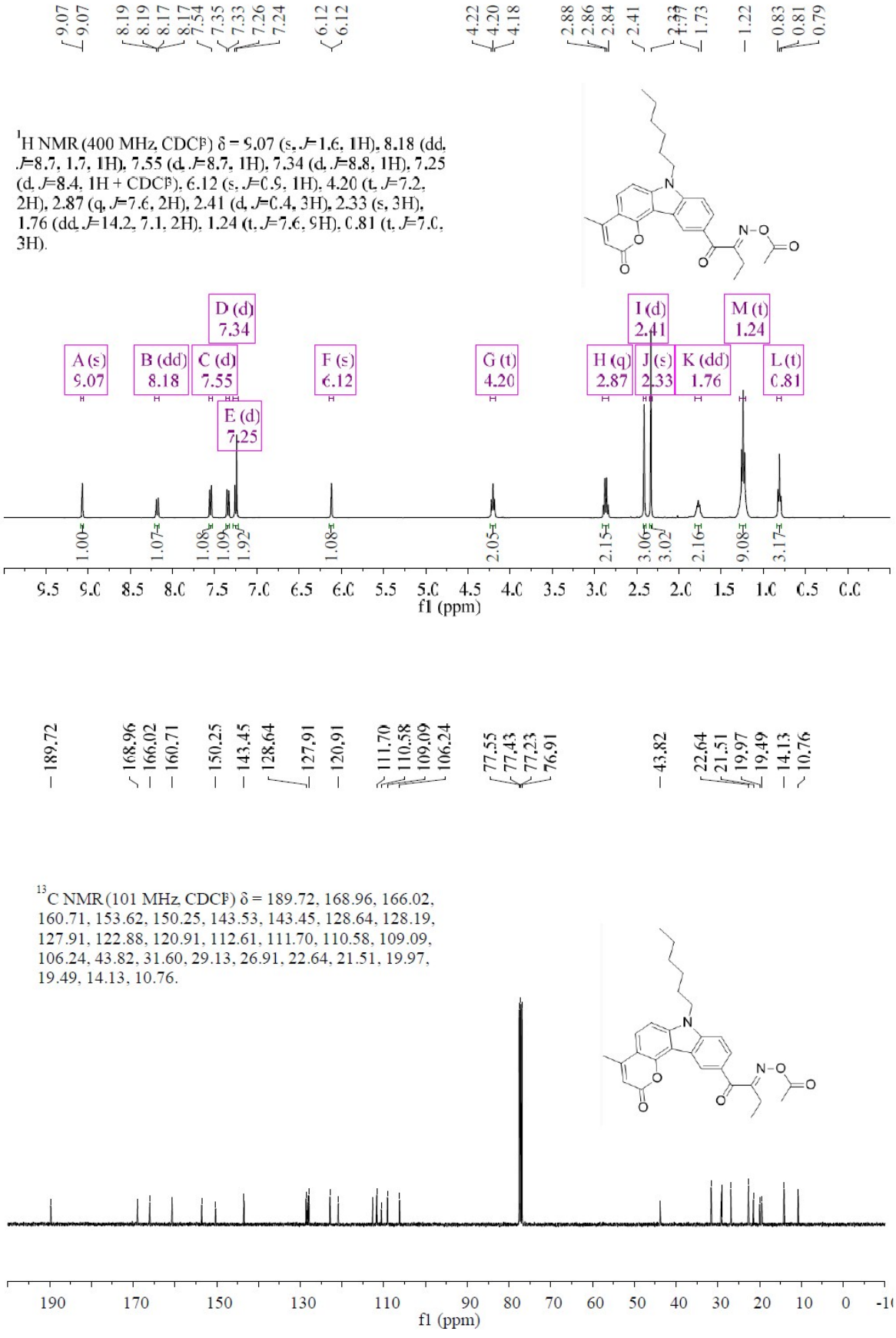

Figure S15. The ^{1}H and ^{13}C NMR spectra of compound (OXE) in $CDCl_3$.

4. References.

1 A. Romani, G. Favaro and F. Masetti, *J. Lumin.*, 1995, **63**, 183-188.

2 J.-P. Malval, M. Jin, L. Balan, R. l. Schneider, D.-L. Versace, H. Chaumeil, A. Defoin and O. Soppera, *J. Phys. Chem. C*, 2010, **114**, 10396-10402.

3 M. Montalti, A. Credi, L. Prodi and M. T. Gandolfi, *Handbook of Photochemistry, Third Ed.*, CRC Press, Boca Raton, 2006.

4 M.Sheik-Bahae, A. A. Said, T. H. Wei, D. J. Hagan and E. W. V. Stryland, *IEEE J. Quant. Electron.* , 1990, **26**, 760.

5 M.Sheik-Bahae, A. A. Said and E. W. V. Stryland, *Opt. Lett.*, 1989, **14**, 955-957.

6 E. W. V. Stryland and M. Sheik-Bahae, in *Characterization Techniques and Tabulations for Organic Nonlinear Materials*, ed. M. G. Kuzyk and C. W. Dirk, Marcel Dekker, Inc.,, 1998, pp. 655-692.

7 P. Sengupta, J. Balaji, S. Banerjee, R. Philip, G. R. Kumar and S. Maiti, *J. Chem. Phys.*, 2000, **112**, 9201-9205.

8 S. Aloise, Z. Pawlowska, C. Ruckebusch, M. Sliwa, J. Dubois, O. Poizat, G. Buntinx, A. Perrier, F. Maurel, P. Jacques, J.-P. Malval, L. Poisson, G. Piani and J. Abe, *Phys. Chem. Chem. Phys.*, 2012, **14**, 1945-1956.

9 M. J. Frisch, Gaussian 09, Revision B.01, in *Gaussian 09, Revision B.01, Gaussian, Inc.,* , Wallingford CT, 2009.